Polymer 49 (2008) 5596–5601

Contents lists available at ScienceDirect

Polymer

journal homepage: www.elsevier.com/locate/polymer

# Self-assembly of rod-terminally tethered three-armed star-shaped coil block copolymer: Investigation of the presence of the branching in the coil to the self-assembled behavior

Yingdong Xia [a], Zhaoyan Sun [a], Tongfei Shi [a], Jizhong Chen [a,*], Lijia An [a,**], Yuxi Jia [b]

[a] State Key Laboratory of Polymer Physics and Chemistry, Changchun Institute of Applied Chemistry, Chinese Academy of Sciences, Changchun 130022, China
[b] School of Materials Science and Engineering, Shandong University, Jinan 250061, China

ARTICLE INFO

*Article history:*
Received 14 July 2008
Received in revised form
11 September 2008
Accepted 12 September 2008
Available online 8 October 2008

*Keywords:*
Self-consistent-field lattice technique
Microphase transition
Rod-terminally tethered three-armed star-shaped coil block copolymer

ABSTRACT

Self-assembled behavior of rod-terminally tethered three-armed star-shaped coil block copolymer melts was studied by applying self-consistent-field lattice techniques in three-dimensional (3D) space. Similar to rod–coil diblock copolymers, five morphologies were observed, i.e., lamellar, perforated lamellar, gyroidlike, cylindrical and sphericallike structures, while the distribution of the morphologies in the phase diagram was dramatically changed with respect to that of rod–coil diblock copolymers. The perforated lamella was replaced by the cylinder when $f_{rod} = 0.45$, and the lamella was replaced by the perforated lamella when $f_{rod} = 0.5$ when the arms $A_1$ and $A_2$ had an equal length and the volume fraction of $A_3$ arm was low enough. Simulations were also performed when the arms $A_1$ and $A_2$ had unequal lengths. These results demonstrate that simple branching in the coil induces interesting microphase transitions.



## 1. Introduction

Much work has been focused on the morphologies and phase behaviors of rod–coil block copolymers due to their fascinating creation of supramolecular architectures with well-defined shapes and functions [1–7]. Especially, the rod–coil block copolymers containing conjugated rod building blocks offer opportunities for engineering novel features, functions and properties into self-assembled structures [8–11]. In the past decades, many interesting microstructures have been observed in experiments [6,12–16], e.g., lamellae, arrowhead lamellae, zigzag lamellae, wave lamellae, strips, honeycombs, and hollow spherical and cylindrical micelles. The driving force of self-assembly of rod–coil block copolymers originates not only from the incompatibility between rodlike and flexible blocks, but also from the tendency of the rod to form orientational order. Taken the simplest rod–coil diblock copolymer for example [17], the block stiffness greatly affects the phase behavior and breaks the symmetry of the phase diagram observed by Masten and Bates [18] when both blocks are flexible, where most of the regions are occupied by the lamellar structure.

The self-assembled structure is in close relationship with the chain architecture and therefore, one can design the architecture of the copolymer chain to explore various self-assembled structures and desired functions. Moreover, due to the rigid block, the self-assembled behavior of the copolymers with the complex chain architecture containing rodlike blocks is different from the copolymers containing only flexible blocks, such as ABA coil–rod–coil and BAB rod–coil–rod triblock copolymers. In addition to varying the number of the blocks in the copolymer chain, another important means is to decorate the coil block of rod–coil block copolymers. In experiments [2,19-23], various rod–coil block copolymers with coil chain branched have been investigated, and the results revealed that the branching in the coil has remarkable effects on the self-assembled behavior. In this paper, we investigate rod-terminally tethered three-armed star-shaped coil block copolymer melts and focus on the effects of the presence of the branching in the coil block on the self-assembled behavior. Furthermore, a rod-terminally tethered three-armed star-shaped coil can be viewed as a unit of a side chain liquid crystalline (SCLC) block copolymer chain [24], and this work is also expected helpful to understand the self-assembly in SCLC block copolymers.

Compared with block copolymers consisting of only flexible blocks, theoretical studies are less developed for rod–coil block copolymers due to the complicated entropy interactions that arise from the asymmetry between the two blocks and the tendency of

* Corresponding author. Tel.: +86 431 85262137; fax: +86 431 85262969.
** Corresponding author. Tel.: +86 431 85262206; fax: +86 431 85262126.
*E-mail addresses:* jzchen@ciac.jl.cn (J. Chen), ljan@ciac.jl.cn (L. An).

0032-3861/$ – see front matter © 2008 Elsevier Ltd. All rights reserved.
doi:10.1016/j.polymer.2008.09.059

the rod to orient itself parallel with the other rods as in liquid crystals. Self-consistent-field theory (SCFT) has been proved a successful way to describe the morphologies of complex flexible block copolymers, such as linear shape [25], star-shape [26,27], H-shape [28], π-shape [29], etc. However, SCFT is not appropriate for the block copolymers containing rigid blocks, because the rigid part does not obey Gaussian statistics. In order to study rod–coil block copolymers, one can use other theories to model the rigid section of the copolymer, while using the Gaussian statistics to describe the flexible block and therefore, a number of modified SCFT calculations have been performed. Matsen and Barrett [30] developed a rod–coil diblock copolymers' model, in which they used Flory's lattice theory to account for orientational interactions between rods, but was restricted to one-dimensional smectic phases. Pryamitsyn and Ganesan [31] predicted the phase diagram for rod–coil block copolymers using a SCFT model where the orientational interactions were modeled by Maier–Saupe interaction. Another way to account for chain rigidity was developed by Li and Gersappe [32]. Incorporating the rotational isomeric state scheme and the self-consistent-field lattice model, they studied the phase diagram of rod–coil diblock copolymer in two-dimensional space. In this paper, we apply our previous SCFT lattice model [17] in three-dimensional space, and the rigid section of the copolymer is described similar to Li and Gersappe method.

As shown in Fig. 1, we present a rod–coil block copolymer containing a three-armed star-shaped coil tethered to one end of the rod to investigate the effects of the branching in the coil on the equilibrium morphologies. We use $f_{A_1}, f_{A_2}, f_{A_3}$ and $f_{rod}$ to denote the volume fraction of $A_1$, $A_2$, $A_3$ and B, respectively. Two situations, i.e., the block copolymers whose arms $A_1$ and $A_2$ have an equal length and unequal lengths, are discussed respectively. A series of phase diagrams are constructed for $f_{rod}$ versus $\chi N$ with different volume fractions of $A_3$ for the first situation, and $f_{A_1}/f_{A_2}$ versus $\chi N$ with different $f_{rod}$ and $f_{A_3}$ for the second situation to study the coil branching effects.

## 2. Theory

We consider a molten system of $n$ rod-terminally tethered three-armed star-shaped coil block copolymers and the total degree of polymerization of each chain is $N$. In order to describe the theory clearly, we consider the entire polymer chain as three parts, i.e., two homopolymers of A with polymerization $f_1N$ and $f_2N$ and an AB rod–coil diblock copolymer with polymerization $f_3N$, connected by a branch point (Fig. 1). Obviously, there is $f_1 = f_{A_1}, f_2 = f_{A_2}$, and $f_3 = f_{A_2} + f_B$. Therefore, the degree of polymerization of the polymer chain can be expressed as $N = f_1N + f_2N + f_3N + 1$ (1 represents the branch point). We suppose that the segments of A block and B block have the same size and each segment occupies one lattice site, thus the total number of the lattice sites is $N_L = n(f_1N + f_2N + f_3N + 1)$. For convenience, we use the segment size of block copolymer as the length unit. The transfer matrix depends only on the chain model used. For this system, we assume that

$$\lambda_{r_{j,s}-r'_{j,s-1}}^{\alpha_{j,s}-\alpha'_{j,s-1}} = \begin{cases} 1, & \alpha_{j,s} = \alpha'_{j,s-1} \\ 0, & \text{otherwise} \end{cases} \tag{1}$$

for the rod section and

$$\lambda_{r_{j,s}-r'_{j,s-1}}^{\alpha_{j,s}-\alpha'_{j,s-1}} = \begin{cases} 0, & \alpha_{j,s} = \alpha'_{j,s-1} \\ 1/(z-1), & \text{otherwise} \end{cases} \tag{2}$$

for the coil section which represents a self-avoiding chain. Here, $r_{j,s}$ and $\alpha_{j,s}$ denote the position and bond orientation of the $s$th segment of the $j$th copolymer, respectively. $r'$ denotes the nearest neighboring site of $r$. $\alpha$ can be any of the allowed bond orientations depending on the lattice model used. We use the cubic lattice model which has six bond orientations and $z$ is the coordination number of the lattice. Our previous work applied the scheme of Scheutjens and Leermakers [33] to deal with linear molecules, and here we treat the branched molecule very similarly. The end segment distribution function $G^{\alpha_s}(r,s|1)$ that gives the statistical weight of all possible walks starting from segment 1, which may locate anywhere in the lattice, and ending at segment $s$ ($s \le f_jN + 1$, $j = 1,2,3$) at site $r$, is evaluated from the following recursive relation:

$$G^{\alpha_s}(r,s|1) = G(r,s) \sum_{r'_{s-1}} \sum_{\alpha'_{s-1}} \lambda_{r_s-r'_{s-1}}^{\alpha_s-\alpha'_{s-1}} G_{s-1}^{\alpha'}(r', s-1|1). \tag{3}$$

The initial condition is $G^{\alpha_1}(r,1|1) = G(r,1)$ for all the values of $\alpha_1$. $G(r,s)$ is the free segment weighting factor and $G(r,s) = \begin{cases} \exp(-\omega_A(r_s)), & s \in A \\ \exp(-\omega_B(r_s)), & s \in B \end{cases}$. Another end segment distribution function $G^{\alpha_s}(r,s|f_jN+1)$ ($j = 1,2,3$) starting from the branch point is evaluated from the following recursive relations:

$$G^{\alpha_s}\left(r,s\middle|f_jN+1\right) = G(r,s) \sum_{r'_{s+1}} \sum_{\alpha'_{s+1}} \lambda_{r'_{s+1}-r_s}^{\alpha'_{s+1}-\alpha_s} G^{\alpha'_{s+1}}\left(r', s+1\middle|f_jN+1\right) \tag{4}$$

with the initial conditions

$$G^{\alpha_{f_jN+1}}\left(r,f_jN+1\middle|f_jN+1\right) = \begin{cases} G^{\alpha_{f_2N+1}}(r,f_2N+1|1)G^{\alpha_{f_3N+1}}(r,f_3N+1|1)/G(r,1) & j=1 \\ G^{\alpha_{f_1N+1}}(r,f_1N+1|1)G^{\alpha_{f_3N+1}}(r,f_3N+1|1)/G(r,1) & j=2 \\ G^{\alpha_{f_2N+1}}(r,f_2N+1|1)G^{\alpha_{f_1N+1}}(r,f_1N+1|1)/G(r,1) & j=3 \end{cases} \tag{5}$$

The form of the free energy function of $F$ (in the unit of kBT) is the same to our previous work [17]

$$F = \sum_r \left\{ \frac{\chi}{z} \sum_{r'} \phi_A(r)\phi_B(r') - \omega_A(r)\phi_A(r) - \omega_B(r)\phi_B(r) - \xi(r) \right. \\ \left. [1 - \phi_A(r) - \phi_B(r)] \right\} - n \ln Q, \tag{6}$$

where

$$Q = \frac{1}{N_L} \frac{1}{z} \sum_{r_N} \sum_{\alpha_N} G^{\alpha_1}(r,1\middle|f_1N+1) \tag{7}$$

is the single chain partition function. Here, $\chi$ is the Flory–Hugginns interaction parameter which measures the incompatibility between A and B segments. $\phi_k(r)$ is the volume fraction field of block species $k$, which is independent of the individual polymer

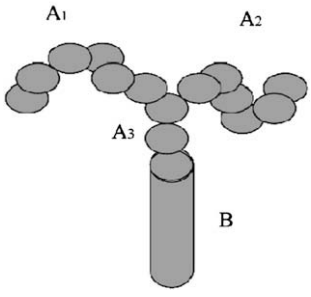


**Fig. 1.** Schematic illustration of rod-terminally tethered three-armed star-shaped coil block copolymer chain. The spheres indicate the segments and the column indicates the rod block.

configurations, and $\omega_k(r)$ is the chemical potential field conjugated to $\phi_k(r)$. $\xi(r)$ is the potential field that ensures the incompressibility of the system, also known as a Lagrange multiplier. Minimizing the free energy function $F$ with respect to $\phi_A(r)$, $\phi_B(r)$, $\omega_A(r)$, $\omega_B(r)$, and $\xi(r)$ leads to the following SCFT equations:

$$\omega_A(r) = \frac{\chi}{z}\sum_{r\prime}\phi_B(r\prime) + \xi(r), \tag{8}$$

$$\omega_B(r) = \frac{\chi}{z}\sum_{r\prime}\phi_A(r\prime) + \xi(r), \tag{9}$$

$$\phi_A(r) + \phi_B(r) = 1, \tag{10}$$

$$\phi_A(r) = \frac{1}{N_L}\frac{1}{z}\frac{n}{Q}\sum_{s\in A}\sum_{\alpha_s}\sum_{j=1,2,3}\frac{G^{\alpha_s}(r,s|1)G^{\alpha_s}\left(r,s\middle|f_jN+1\right)}{G(r,s)}, \tag{11}$$

$$\phi_B(r) = \frac{1}{N_L}\frac{1}{z}\frac{n}{Q}\sum_{s\in B}\sum_{\alpha_s}\sum_{j=1,2,3}\frac{G^{\alpha_s}(r,s|1)G^{\alpha_s}\left(r,s\middle|f_jN+1\right)}{G(r,s)}. \tag{12}$$

In our calculations, the real space method is implemented to solve the SCF equations in a cubic lattice with periodic boundary conditions, which is similar to our previous paper [17,34,35]. To prevent bias of the resulting morphologies, our calculations are initiated with different random generated fields. The calculation stops when the free energy changes within a tolerance of $10^{-8}$. The morphologies obtained correspond to either a stable or a metastable state. By comparing the free energy of the system, the relative stability of the morphologies can be assessed.

## 3. Results and discussion

In our studies, the polymer chain architecture is shown in Fig. 1. Thus, the ordered morphologies of the rod-terminally tethered three-armed star-shaped coil block copolymer depend on the following tunable parameters: $f_{rod}$ (the volume fraction of the rod block), $f_{A_j}$ (the volume fraction of the three flexible arms, respectively, $j = 1,2,3$ as shown in Fig. 1), $\chi$ (the Flory–Huggins interaction parameter depending on the temperature), and $N$ (the total degree of polymerization of the block copolymer chain). Obviously, only five of these parameters are independent variables. Two situations are considered in our calculations. One is that the block copolymers whose arms $A_1$ and $A_2$ have an equal length, and a set of phase diagrams are constructed in $f_{rod}$ versus $\chi N$ with respect to different $f_{A_3}$. The other situation is that the arms $A_1$ and $A_2$ have unequal lengths, and a set of phase diagrams are constructed in $f_{A_1}/f_{A_2}$ versus $\chi N$ with respect to different $f_{rod}$ and $f_{A_3}$. All these phase diagrams are compared with the diagram of rod–coil diblock copolymers [17] to examine the effects of the branching in the coil block on self-assembled structures. Our calculations are preformed in $N_L = 40^3$ and $N_L = 60^3$ lattices to make sure that the emergence of the self-assembled structures is not constrained by system size, and the degree of polymerization is 20 the same as our previous work of the rod–coil diblock copolymer [17]. Below we present details on the calculated results.

In the first situation, we keep $f_{A_1}/f_{A_2} = 1.0$, and then the self-assembled structures are investigated by varying $f_{rod}$ and $\chi N$ with respect to different $f_{A_3}$ as shown in Fig. 2. The corresponding phase diagrams are shown in Fig. 3. Because the predetermined degree of polymerization is kept 20 and $f_{A_1}/f_{A_2}$ is kept 1.0 in our calculations, the phase diagrams in Fig. 3(a) and (c) are plotted in the rod volume fraction ranging from 0.25 to 0.75 with interval 0.1 and the phase diagrams in (b) and (d) are plotted in the rod volume fraction ranging from 0.2 to 0.8 with interval 0.1. In order to investigate the influence of the changing architecture of the flexible block from linear to a branched one, the phase diagram of the rod–coil diblock copolymer is shown in Fig. 4(a), [17] to make comparison. Furthermore, we calculate the self-assembled morphologies of the rod–coil diblock copolymer in detail whose rod fraction $f_{rod}$ ranges from 0.25 to 0.75 with interval 0.1. As is shown in Fig. 4(b), we find the perforated lamellar structure stable between the regions of lamellar and cylindrical phases, which is in consistent with the work of Horsch et al. [36]. The perforated lamellar structure may result from the competition between the rods attempting to maximize their contact with other rods to minimize energy and the coils attempting to minimize their free volume to maximize entropy [17,36].

As shown in Fig. 3, there are five stable structures observed in our calculations similar to the rod–coil diblock copolymer [17,36], i.e., lamellar, perforated lamellar, gyroidlike, cylindrical and sphericallike structures, which indicates that the difference of chain architectures does not give rise to novel stable phase structures. We also examine the orientations of the rods in the self-assembled structures like our previous work [17], and find that the branching in the flexible component does not affect the arrangement fashion of the rods, i.e., the rods aligning along a common direction in the lamellar and perforated lamellar structure and packing in a complex interdigitated bilayer fashion in the cylindrical structure. When $f_{A_3} = 0.0$, two coils are tethered to the same end of the rod as shown in Fig. 2. We find that the cylindrical structure is stable when $f_{rod}$ equals to 0.45 (shown in Fig. 3(a)), while the perforated lamellar structure is stable for the same rod volume fraction in the phase diagram of the rod–coil diblock copolymer (shown in Fig. 4(b)). This difference can be attributed to the interplay between the elastic stretching free energies of the coil component and the interfacial energy between rod and coil segments. The rods in the perforated lamellar structure align along a common direction due to the rigid conformation of the rod segments. As the linear coil block becomes a branched one, entropy associated with the excluded volume of the flexible component is decreased sharply when the rods are oriented along a common direction, leading to the rods packing in a complex interdigitated

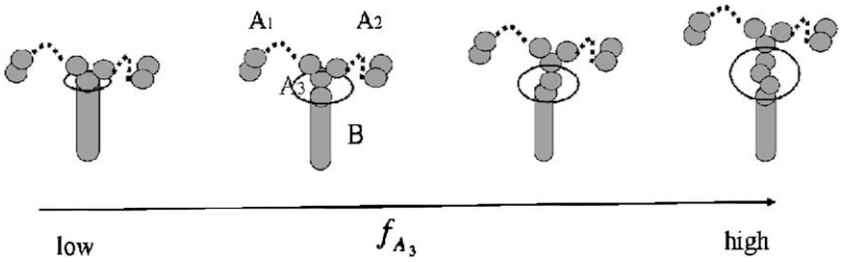


**Fig. 2.** Process of structural variations of the copolymer studied ($f_{A_1}/f_{A_2} = 1.0$). The changing parts are marked by ellipses.

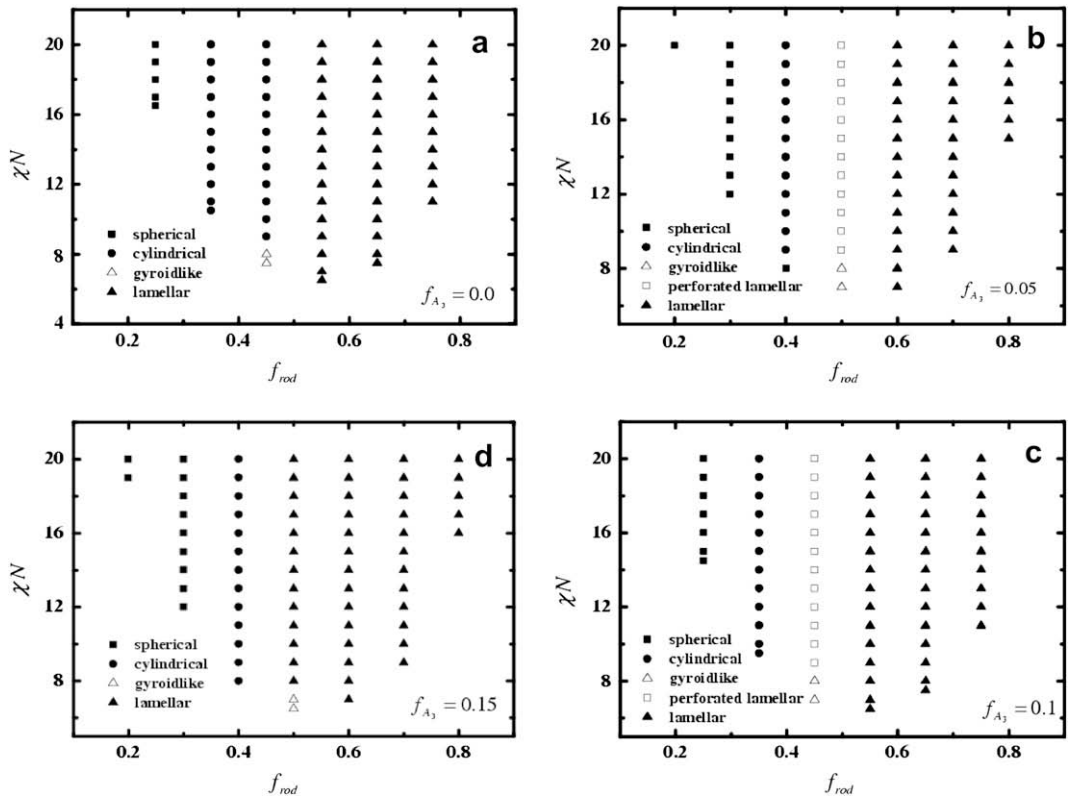


**Fig. 3.** Phase diagrams plotted in $f_{rod}$ versus $\chi N$ for symmetric ($f_{A_1}/f_{A_2}$ 1.0) rod-terminally tethered three-armed star-shaped coil block copolymers for (a) $f_{A_3} = 0.0$; (b) $f_{A_3} = 0.05$; (c) $f_{A_3} = 0.1$; (d) $f_{A_3} = 0.15$.

bilayer fashion to form the cylindrical phase to decrease the interfacial grafting density of the separating rod and coil segments to maximize entropy for $f_{rod} = 0.45$. Similarly, when $f_{A_3} = 0.05$, the stable perforated lamellar phase is observed for $f_{rod} = 0.5$ in Fig. 3(b), where the lamellar phase is the stable one in Fig. 4(a). The rods in the perforated lamellar phase and the lamellar phase have the same fashion, where all rods attempt to align along a common direction to maximize their contact with other rods to minimize energy. When the rod fraction is lowered from that of the lamellar phase, the sheetlike rod domains would be perforated to lower the grafting density to increase the entropy. The branching of the coil component results in an increase of the elastic energy of the coil and a decrease in entropy, which in turn allows this transition occurring at high rod fraction. The effects of the branching in the coil diminish with the volume fraction of $A_3$ arm increasing. As shown in Fig. 3(c) and (d), the phase diagrams of the rod-terminally tethered three-armed star-shaped coil block copolymer are found to be similar to that of the rod–coil diblock copolymer. When the volume fraction of $A_3$ arm is high, the distance between the anchor point (the grafting point of the rod and coil segments) and the branch point is increased as shown in Fig. 2, which results in a weakening in effects of the branching chain architecture on the interplay between the elastic stretching free energies of the coil component and the interfacial energy between rod and coil segments. The above order–order phase transitions can be shown in Fig. 5. Furthermore, we find that the effects of the branching in the coil can be close to negligible at high rod volume fraction. As shown in Fig. 3, the lamella is the only stable structure for $f_{rod} > 0.5$,

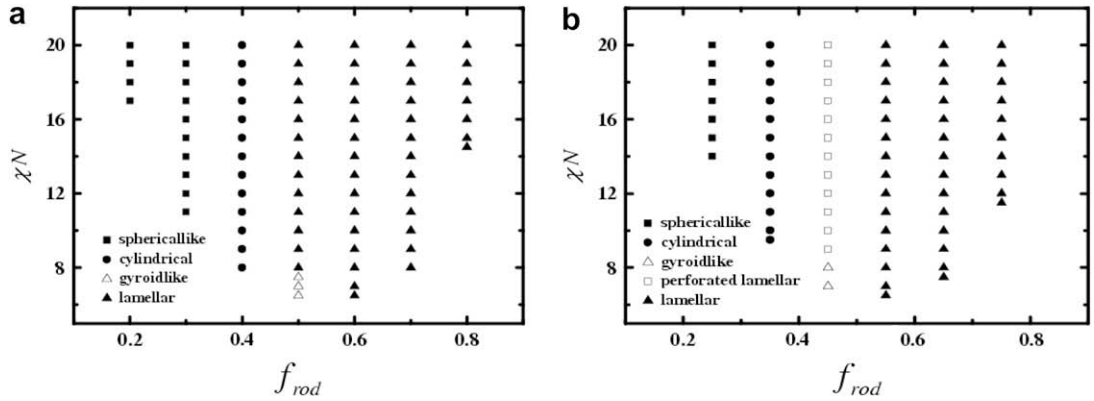


**Fig. 4.** Phase diagrams plotted in $f_{rod}$ versus $\chi N$ for the rod–coil diblock copolymer for (a) $f_{rod}$ ranging from 0.2 to 0.8 [15]; (b) $f_{rod}$ ranging from 0.25 to 0.75.

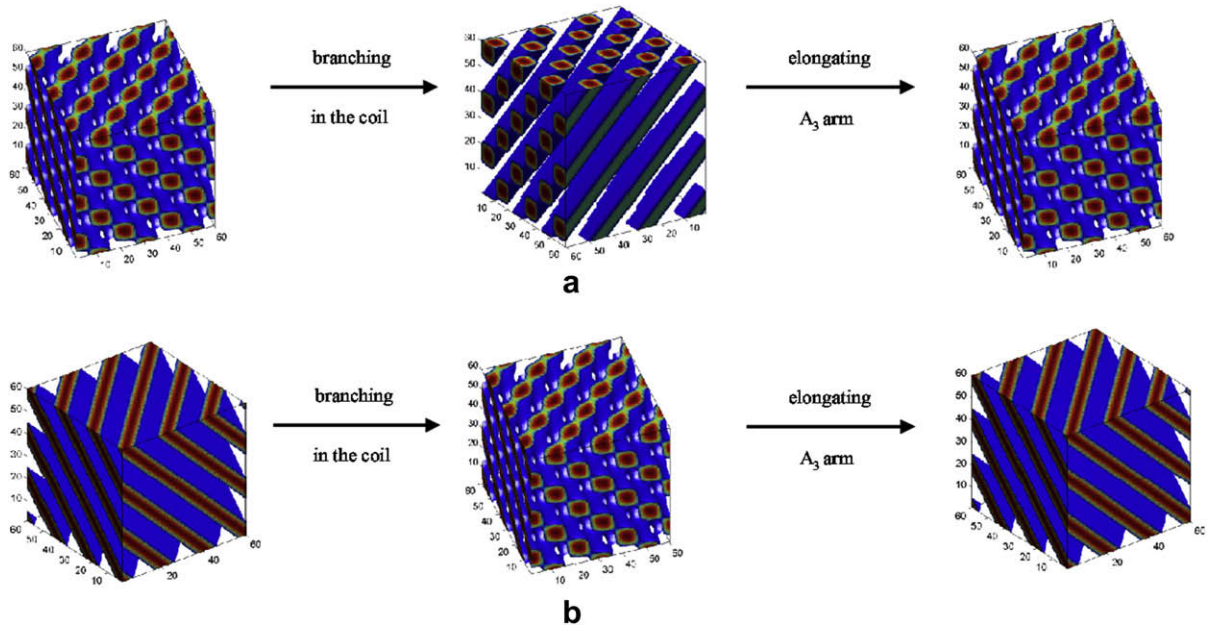


**Fig. 5.** Phase transitions for (a) perforated lamella – cylinder – perforated lamella when $f_{rod} = 0.45$, and (b) lamella – perforated lamella – lamella when $f_{rod} = 0.5$.

which is the same to the diagram of the rod–coil diblock copolymer. Moreover, the interesting zigzag structure observed in experiments [13] and theoretical works [17,32] of rod–coil diblock copolymers also emerges for $f_{rod} = 0.6$ with respect to the volume fractions of $A_3$ arm in our calculations, which also indicates that the branching of the flexible part of the rod–coil block copolymer has no effect on self-assembled behavior when the volume fraction of the rigid block is high enough.

In order to study the coil branching effects when the block copolymer whose arms $A_1$ and $A_2$ have unequal lengths, we move the position of the branch point as shown in Fig. 6. The architecture of the chain is varied from a rod-terminally tethered three-armed star-shaped coil ($f_{A_1}/f_{A_2} = 1.0$) block copolymer to a rod–coil diblock one ($f_{A_1}/f_{A_2} = 0.0$). The corresponding variations of the number of segments $A_1$ and $A_2$ and the ratios of them calculated in our present work are shown in Table 1. The parameters $f_{rod} = 0.45$, $f_{A_3} = 0.0$ and $f_{rod} = 0.5$, $f_{A_3} = 0.05$ are considered in our calculations, where the effects of the branching in the coil on the equilibrium morphologies are observed as discussed above. Then, the phase diagrams are constructed in $f_{A_1}/f_{A_2}$ versus $\chi N$ as shown in Fig. 7. For $f_{rod} = 0.45$ and $f_{A_3} = 0.0$, as the position of the branch point moving, the cylindrical phase becomes unstable and the perforated lamellar phase has lower free energies (the effects of the branching diminish) when $f_{A_1}/f_{A_2} < 3/7$ as shown in Fig. 7(a). For $f_{rod} = 0.5$ and $f_{A_3} = 0.05$, the effects of the branching in the coil can also be observed (i.e., the perforated lamella is the stable phase) even when the ratio of $f_{A_1}/f_{A_2}$ is very low ($f_{A_1}/f_{A_2} = 1/7$) as shown in Fig. 7(b).

**Table 1**
The variations of the number of segments $A_1$ and $A_2$ and the ratios of them with the branch point moving when (a) $f_{rod} = 0.45$, $f_{A_3} = 0.0$; (b) $f_{rod} = 0.5$, $f_{A_3} = 0.05$.

| $f_{A_1}N$ | $f_{A_2}N$ | $f_{A_1}/f_{A_2}$ |
|---|---|---|
| (a) $f_{rod} = 0.45$, $f_{A_3} = 0.0$ | | |
| 5 | 5 | 5/5 |
| 4 | 6 | 4/6 |
| 3 | 7 | 3/7 |
| 2 | 8 | 2/8 |
| 1 | 9 | 1/9 |
| 0 | 10 | 0 |
| (b) $f_{rod} = 0.5$, $f_{A_3} = 0.05$ | | |
| 4 | 4 | 4/4 |
| 3 | 5 | 3/5 |
| 2 | 6 | 2/6 |
| 1 | 7 | 1/7 |
| 0 | 8 | 0 |

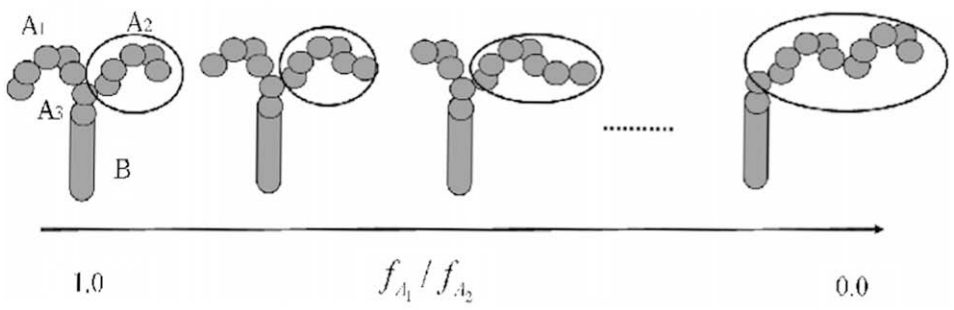


**Fig. 6.** Process of varying a rod-terminally tethered three-armed star-shaped coil block copolymer to a rod–coil diblock one. The changing parts are marked by ellipses.

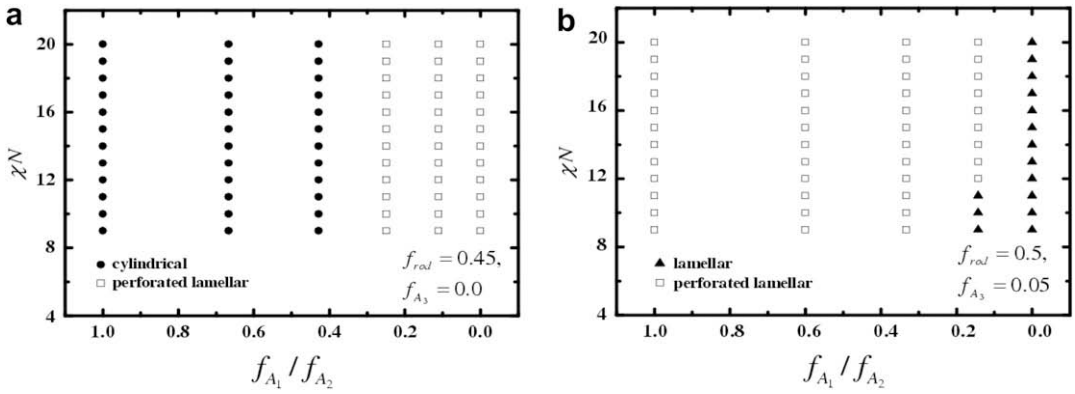


**Fig. 7.** Phase diagrams of the rod-terminally tethered three-armed star-shaped coil block copolymers plotted in $f_{A_1}/f_{A_2}$ versus $\chi N$ for (a) $f_{rod} = 0.45$, $f_{A_3} = 0.0$; (b) $f_{rod} = 0.5$, $f_{A_3} = 0.05$.

## 4. Conclusion

As an extension of our previous works, the self-assembled behavior of rod-terminally tethered three-armed star-shaped coil block copolymer melts is investigated by applying SCF lattice techniques in three-dimensional space. Similar to rod–coil diblock copolymers, five morphologies are observed for this block copolymer in our calculations, i.e., lamellar, perforated lamellar, gyroid-like, cylindrical and sphericallike structures. The notable characteristic of this block copolymer is the presence of the branching in the coil block which imposes significant effects on the phase behavior. When $A_1$ and $A_2$ have an equal length and the volume fraction of $A_3$ is low enough, i.e., $f_{A_3} < 0.1$, the perforated lamellar phase is replaced by the cylindrical phase when $f_{rod} = 0.45$ and the lamellar phase is replaced by the perforated lamellar phase at $f_{rod} = 0.5$. When the distance between the anchor point and the branch point is increased (i.e., $f_{A_3} \geq 0.1$), the effects of the coil branching on the morphologies can be neglected. Furthermore, for the block copolymer whose arms $A_1$ and $A_2$ have unequal lengths, $f_{rod} = 0.45$ and $f_{A_3} = 0.0$, the branch effect exits at $f_{A_1}/f_{A_2} < 3/7$ where the cylindrical phase becomes unstable and the perforated lamellar phase has lower free energies. For $f_{rod} = 0.5$ and $f_{A_3} = 0.05$, the branch effect can be observed even when $f_{A_1}/f_{A_2}$ is very low ($f_{A_1}/f_{A_2} = 1/7$) where the perforated lamella is the stable phase. These simulation results reveal that the effects of the coil branching on the self-assembled behavior provide an efficient way to realize the desired microphases, and are expected to provide guidance for the design and synthesis of block copolymers.

Our model and results should encourage the search for the phase behavior of SCLC block copolymers, for if more rods are tethered to the flexible backbone, the block copolymer becomes a SCLC one [24]. The SCLC block copolymers are a special class of liquid crystalline polymers exhibiting rich self-assembly characteristics and potential use in photoelectric display devices and high strength fibers. By applying our lattice self-consistent field model, tuning the parameters that affect the self-assembly morphologies, such as the degree of polymerization, the length of the flexible spacer, the volume fraction of the mosogenic units, etc, the phase behavior of SCLC block copolymers is expected to be explored in three-dimensional space.

## Acknowledgments

This work is supported by the National Natural Science Foundation of China (20804047, 20574070, 20774096) Programs and the Fund for Creative Research Groups (50621302), and subsidized by the Special Funds for National Basic Research Program of China (2005CB623800).

## References

[1] Lehn JM. Supramolecular chemistry. Weinheim, Germany: VCH; 1995.
[2] Stupp SI, LeBonheur V, Walker K, Li LS, Huggins KE, Keser M, et al. Science 1997;276:384.
[3] Park C, Yoon J, Thomas EL. Polymer 2003;44:6725.
[4] Nicol E, Niepceron F, Bonnans-Plaisance C, Durand D. Polymer 2005;46:2020.
[5] Oesterbacka R, An CP, Jiang XM, Vardeny ZV. Science 2000;287:839.
[6] Laicer CST, Mrozek RA. Polymer 2007;48:1316.
[7] Baeurle SA, Hotta A, Gusev AA. Polymer 2006;47:6243.
[8] Jenekhe SA, Chen XL. Science 1998;279:1903.
[9] Jenekhe SA, Chen XL. J Phys Chem B 2000;104:6332.
[10] Minich EA, Nowak AP, Deming TJ, Pochan DJ. Polymer 2004;45:1951.
[11] Chen ZR, Kornfield JA. Polymer 1998;39:4679.
[12] Chen JT, Thomas EL, Ober CK, Hwang SS. Macromolecules 1995;28:1688.
[13] Chen JT, Thomas EL, Ober CK, Hwang SS. Science 1997;273:343.
[14] Radzilowski LH, Carragher BO, Stupp SI. Macromolecules 1997;30:2110.
[15] Oh NK, Zin WC, Hwan J, Lee M. Polymer 2006;47:5275.
[16] Lee M, Cho BK, Ihn KJ, Lee WK, Oh NK, Zin WC. J Am Chem Soc 2001;123:4647.
[17] Chen JZ, Zhang CX, Sun ZY, Zheng YS, An LJ. J Chem Phys 2006;124:104907.
[18] Matsen MW, Bates FS. Macromolecules 1996;29:1091.
[19] Yoo YS, Choi JH. J Am Chem Soc 2004;126:6294.
[20] Lee M, Oh NK, Zin WC. Chem Commun 1996:1787.
[21] Pralle MU, Whitaker CM, Braun PV, Stupp SI. Macromolecules 2000;33:3550.
[22] Tew GN, Pralle MU, Stupp SI. Angew Chem Int Ed 2000;39:517.
[23] Tew GN, Pralle MU, Stupp SI. J Am Chem Soc 1999;121:9852.
[24] Shah M, Pryamitsyn V, Ganesan V. Macromolecules 2008;41:218.
[25] (a) Matsen MW, Schick M. Phys Rev Lett 1994;72:2660;
(b) Tang P, Qiu F, Zhang HD, Yang YL. Phys Rev E 2004;69:031803;
(c) Drolet F, Fredrickson GH. Phys Rev Lett 1999;83:4317.
[26] (a) Tang P, Qiu F, Zhang HD, Yang YL. J Phys Chem B 2004;108:8434;
(b) Matsen MW, Schick M. Phys Rev Lett 1994;27:6761.
[27] Wang R, Xu TT. Polymer 2007;48:4601.
[28] Ye XG, Yu XF, Sun ZY, An LJ. J Phys Chem B 2006;110:12042.
[29] Ye XG, Shi TF, Lu ZY, Zhang CX, Sun ZY, An LJ. Macromolecules 2005;38:8853.
[30] Matsen MW, Barrett C. J Chem Phys 1998;109:4108.
[31] Pryamitsyn V, Ganesan V. J Chem Phys 2004;120:5824.
[32] Li WT, Gersappe D. Macromolecules 2001;34:6783.
[33] Leermakers FAM, Scheutjens JMHM. J Chem Phys 1988;89:3264.
[34] Chen JZ, Zhang CX, Sun ZY, An LJ, Tong Z. J Chem Phys 2007;127:024105.
[35] Chen JZ, Sun ZY, Zhang CX, An LJ, Tong Z. J Chem Phys 2008;128:074904.
[36] Horsch MA, Zhang ZL, Glotzer SC. Phys Rev Lett 2005;95:056105.